Hindawi
Journal of Advanced Transportation
Volume 2018, Article ID 2029586, 14 pages
https://doi.org/10.1155/2018/2029586

Research Article

Capacity-Constrained Contraflow Adaption for Lane Reconfiguration in Evacuation Planning

Wu Ni,[1] Wenbo Li,[2] Hailei Wang,[2] Chengxin Xiong,[1] and Dan Guo[1]

[1]*School of Computer and Information, Hefei University of Technology, Hefei 230009, China*
[2]*Institute of Technology Innovation, Hefei Institutes of Physical Science, Chinese Academy of Sciences, Hefei 230088, China*

Correspondence should be addressed to Wenbo Li; wbli@iim.ac.cn

Received 22 January 2018; Revised 30 March 2018; Accepted 15 April 2018; Published 27 June 2018

Academic Editor: Ludovic Leclercq

This paper presents a heuristic contraflow-based reconfiguration evacuation algorithm, which is named Capacity-Constrained Contraflow Adaption (CC-Adap). First, it effectively calculates optimal candidate routes for evacuation. Second, an evaluation method is proposed for estimating these candidate routes. Third, CC-Adap utilizes a contraflow-based method to reconfigure the evacuation routes to improve capacity constraints. Fourth, traffic conditions are updated in real time. Fifth, CC-Adap reuses historical evacuation routes to reduce the computational cost and accelerate the evacuation process. Experimental results show that CC-Adap generates high-performing evacuation strategies and can be used to tackle large-scale evacuation planning.

1. Introduction

In recent years, both natural and man-made disasters have posed serious threats to humans, such as Hurricane Andrew [1], Hurricane Katrina [2], the "9/11" terrorist attack event [3], and 2011 Tohoku Earthquake Tsunami [4]. Effective evacuation plans are necessary for saving lives and minimizing casualties. The most important objective of an effective evacuation plan is to transfer evacuees to safe areas as quickly as possible. However, dynamic factors make this objective complicated to achieve. For example, the original intention in designing a transportation network is not to address the sharp increase of traffic flow when an emergency occurs [5]. The number of evacuees might far exceed the road capacity, thereby making evacuation route planning a computational challenge.

A well-known routing algorithm, namely, Capacity-Constrained Route Planner (CCRP) [1], was proposed for tackling evacuation route planning. CCRP models the capacity constraints of roads and intersections and selects the shortest paths for evacuation. Later, two heuristics, namely, Intelligent Load Reduction (ILR) and Incremental Data Structure (IDS), were introduced to improve the algorithm's performance [6]. Although routing algorithms can effectively solve mid-size traffic evacuation problems [6], they might not be effective for large-scale evacuation scenarios with massive number of evacuees, which might lead to heavy traffic congestion, owing to capacity constraints. Contraflow-based methods are considered effective techniques for alleviating traffic congestion [2]. Contraflow-based methods reconfigure the edges in the ideal direction and reallocate edge capacity to reduce the evacuation time. For example, Kim et al. presented a heuristic approach that combines a Greedy method and a contraflow-based method for implementing transportation network reconfiguration and, to some extent, minimizing the total evacuation time [2]. However, finding an optimal contraflow plan for reconfiguring network is computationally challenging because we must enumerate all possible combinations of edges in the exhaustive search space [2]. Moreover, it takes a considerable amount of time to evaluate these contraflow candidates by calculating the evacuation time.

In this paper, we propose a Capacity-Constrained Contraflow Adaption (CC-Adap) algorithm for effective evacuation. CC-Adap consists of five steps. First, we utilize an evacuation algorithm to generate optimal candidate routes for evacuees, which finds the routes with maximal flow rate among all the available routes from source vertices to sink vertices. Second, we propose an evaluation method for heuristically

evaluating the candidate routes' capabilities based on the traffic conditions and determining the appropriate routes for evacuation. Then, we implement a contraflow-based method for optimizing the routes' performances and reducing traffic congestion. Next, traffic conditions are updated in real time to make the route planning more practical. Finally, CC-Adap reuses the historical evacuation routes before calculating the available routes at each new time step. Experimental results indicate that CC-Adap boosts performance in evacuation route planning.

The remainder of this paper is organized as follows: Section 2 introduces some related works. Section 3 defines the transportation network and contraflow problem. Section 4 details the CC-Adap evacuation algorithm. Experimental results and analysis are presented in Section 5. Section 6 presents the conclusions of this paper.

2. Related Work

To the best of our knowledge, the existing methods can be divided into descriptive and prescriptive approaches [5]. Descriptive approaches aim at mimicking real emergency evacuations based on the simulation of the traffic situations and drivers' behaviours, while prescriptive methods mainly focus on providing a high-performing evacuation plan with minimum evacuation time.

2.1. Descriptive Methods. The aim of descriptive methods is to simulate traffic evacuation situations as vividly as possible. Many traffic evacuation simulation tools have been proven to be capable of solving complex traffic evacuation problems, including MITSIMLab [7], VISSIM [8], MATSim [9], DynusT and DYNASMART [10], and AIMSUN [11]. In addition, some simulation methods utilize multimodel integration methods to simulate evacuees' behaviours during evacuation and combine various existing evacuation methods for more realistic traffic simulation. For example, Pan et al. implemented a simulation framework for classifying evacuees' behaviours into locomotion, steering, and social for evacuation analysis [12]. Wu and Huang combined a control volume model and a flow merging hypothesis to simulate evacuees' behaviours in high-rise building evacuation situations [13]. Noh et al. considered different behaviours of heterogeneous evacuees in building evacuation [14]. They presented a partially dedicated evacuation strategy that divides evacuees into heterogeneous groups, assigns corresponding routes based on a flow model and a simulation optimization approach, and, to some extent, minimizes the average evacuation time [14]. Beloglazov et al. studied the behaviours of people in wildfire evacuation and integrated traffic simulator, wildfire simulator, and behaviour simulator to define the risk metric and provided detailed plan of how evacuation unfold [15]. Yuan et al. constructed a multilevel agent decision model for simulating driver's behaviours and determining actions for each agent [16]. These descriptive methods can achieve satisfactory performance in traffic evacuation for local communities. However, most exhibit poor generalization performance owing to high computational complexity.

2.2. Prescriptive Methods. Prescriptive methods typically provide suggested schedules for evacuation planners, aiming at reducing traffic congestion and minimizing total evacuation time. Zeng and Wang made a small modification to CCRP to improve the performance, which gives priority to longer evacuation routes for evacuating evacuees [17]. Kang et al. calculated the Dijkstra shortest evacuation paths and chose the best one for evacuees based on current traffic conditions [18]. Shahabi and Wilson proposed a Capacity-Aware Shortest Path Evacuation Routing (CASPER) framework for emergency traffic evacuation, which utilizes an advanced traffic model and an intelligent routing algorithm to calculate the optimal evacuation plan for evacuees [5]. Khan et al. used the Intelligent Transportation System (ITS) to compute the maximum traffic flow and the routes with least traffic congestion towards safe places for evacuees based on real-time traffic conditions [19]. Pourrahmani et al. considered the uncertain evacuee demand at the pick-up source points by utilizing fuzzy credibility theory to present a genetic algorithm (GA) for handling the stated evacuation problem [20]. Chen et al. implemented a distribution Load-balancing Emergency Guiding System (LEGS) to assign the fastest paths to transfer evacuees to the exits according to the capacity constraints and concurrent movement of evacuees [21]. Ikeda and Inoue proposed a Multi-Objective Genetic Algorithm (MOGA) to evaluate evacuation routes by considering route distance and evacuation time to select optimal evacuation routes [22]. Heydar et al. divided the transportation network into pedestrian network and vehicular network, where pedestrians were assigned the shortest routes to the safe areas in pedestrian network and vehicles transferred evacuees to designated shelters in vehicular network [23]. These prescriptive methods have demonstrated the feasibility of calculating evacuation strategies for traffic evacuation. However, the performances of these prescriptive methods are usually limited owing to the capacity constraints of road segments and intersections.

Previous works [24–27] have considered the benefits of contraflow-based methods on evacuation planning. In addition, in the literatures, the optimality of evacuation planning by integrating contraflow-based methods has been validated. For example, Xie et al. designed a bilevel framework for optimizing network evacuation performance, in which the lower level solves the traffic assignment problem and the upper level integrates a contraflow method with crossing elimination strategies to optimize the traffic assignment [28]. Wang et al. implemented a multiobjective optimization model to determine the evacuation priorities and setup time for doing the contraflow operations [3]. Even et al. implemented a conflict-based path-generation algorithm to simultaneously guide the evacuation and select the to-be-reversed roads [29]. Kim et al. presented a Bottleneck Relief (BR) approach that iteratively flips min-cut edges based on the theorem in [30] for solving massive traffic evacuation problems [2].

Above-mentioned contraflow-based methods are selected to generate contraflow strategy that can tackle capacity constraints effectively [2, 3, 24–29]. However, there are two difficulties in calculating the appropriate contraflow strategy

for the complex traffic system. The first difficulty is that it is a time-consuming task to determine the appropriate to-be-reversed edges in the complex traffic network [2, 24, 25]. The second difficulty is that it is difficult to determine the ideal direction of these edges after being reversed [2, 3, 28, 29]. Thus, it is vital for the planners to find an appropriate contraflow strategy that could overcome these two difficulties.

So, this paper presents a prescriptive algorithm to generate appropriate contraflow strategy and optimal evacuation plan. For the first difficulty, the presented algorithm utilizes Greedy method and iterative optimization technique to select the to-be-reversed edges on the evacuation routes. For the second difficulty, the ideal direction of these to-be-reversed edges is determined by the traffic flow on the evacuation routes.

3. Modeling and Problem Formulation

Various methods, such as simulation [13–15], classification network [23], and mathematical modeling [1, 2], are used to formulate the evacuation situations. In this paper, the mathematical graph is used to describe the traffic evacuation situations [1, 2, 5, 6, 17].

3.1. Network Modeling. Suppose we are given a multisource and multisink transportation network $G(V, E)$, where $V = \{V_S, V_M, V_D\}$ and E, respectively, represent the sets of vertices and edges. Here, V_S is the source vertex set, V_M is the transition vertex set, and V_D is the sink vertex set. The definitions of the vertices and edges are given as follows:

(i) Each vertex $V_i \in V$ has a maximal vertex capacity $V_{i,MCap}$ and each source vertex $V_s \in V_S$ has an extra initial occupancy $V_{s,Occ}$, which represents the number of evacuees. For each sink vertex $V_d \in V_D$, the value of $V_{d,MCap}$ can be set according to the actual demand. In this paper, $V_{d,MCap}$ of each sink vertex is set to *infinity*.

(ii) Each edge $e^{\langle V_i,V_j\rangle} \in E$ has a maximal edge capacity $e^{\langle V_i,V_j\rangle}_{MCap}$, a travel time $e^{\langle V_i,V_j\rangle}_{traT}$, and an initial direction. $e^{\langle V_i,V_j\rangle}_{MCap}$ is the number of evacuees (e.g., residents or vehicles) that can pass per unit period. The edge direction is initialized according to the real road conditions. $e^{\langle V_i,V_j\rangle}_{traT}$ is the time cost when evacuees pass edge $e^{\langle V_i,V_j\rangle}$. Various factors should be considered when formulating edge travel time, such as road length, traffic flow, and drivers' behaviours. Many works have studied the relationship between these factors and edge travel time [13–15, 17]. This paper focuses on the impact of road length and traffic flow on the edge travel time. Considering the emergency situations, the traffic flow on the edges should be limited by the maximal edge capacity. Thus, the evacuees can use maximal speed passing one given edge when the traffic flow does not exceed the maximal edge capacity. In other words, more evacuees can be evacuated to safe area using this strategy in the minimum time. According to this, the edge travel time in the transportation network model is determined by the length and the maximal edge capacity of one given road.

There are different traffic elements in transportation network including buildings, crossroads, playgrounds, shelters, and parks. Buildings, crossroads, and playgrounds are the most common traffic elements in transportation network. Figure 1 illustrates the modeling results of the buildings, the crossroad, and the playground. Firstly, the buildings are modeled as source vertex. Secondly, the crossroad is modeled as transition vertex. Thirdly, the playground is modeled as sink vertex. The edges of the vertices are modeled according to the traffic configuration. As for the other traffic elements, they are modeled similar to these three common traffic elements shown in Figure 1.

The objective of transportation evacuation is to find an optimal plan with minimum evacuation time. The objective function is defined in

$$EvaT = \min \left[\max_{r\in RS}(ts + c(r))\right]$$
$$\text{s.t.} \begin{cases} ① \sum_{r\in RS} f(r) = V_{s,Occ} \quad V_s \in V_S, V_s \in r \\ ② \sum_{V_d\in V_D}\sum_{r\in RS} f(r) = \sum_{V_s\in V_S} V_{s,Occ} \quad V_d \in r \\ ③ \ V_{i,MCap} \geq 0; e^{\langle V_i,V_j\rangle}_{MCap} \geq 0; V^{t_i}_{i,cap} \geq 0; e^{(\langle V_i,V_j\rangle,t_i)}_{cap} \geq 0 \end{cases} \tag{1}$$

$EvaT$ is the total evacuation time, ts is the initial time step when a group of evacuees leaves the source vertex, RS is the to-be-solved evacuation route set, and r is an evacuation route in RS.

$c(r)$ is used to calculate the travel time of route r when evacuees pass through the edges along route r and is expressed in (2). For route $r\langle V_0 - V_1 - \cdots - V_n - \cdots - V_N\rangle$, where V_n is the nth vertex of route r, V_0 is the source vertex of route r, and V_N is the sink vertex of route r. $e^{\langle V_{n-1},V_n\rangle}_{traT}$ means the travel time from vertex V_{n-1} to vertex V_n along route r.

$$c(r) = \sum_{n=1}^{N} e^{\langle V_{n-1},V_n\rangle}_{traT} \quad \forall e^{\langle V_{n-1},V_n\rangle} \in r \tag{2}$$

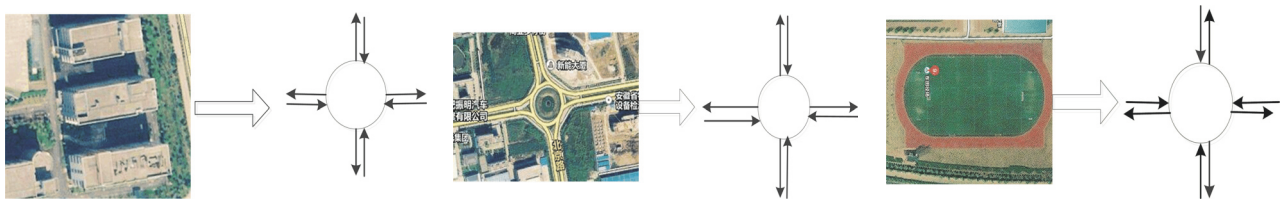

(a) Source vertex (b) Transition vertex (c) Sink vertex

Figure 1: Illustration of the vertices and edges.

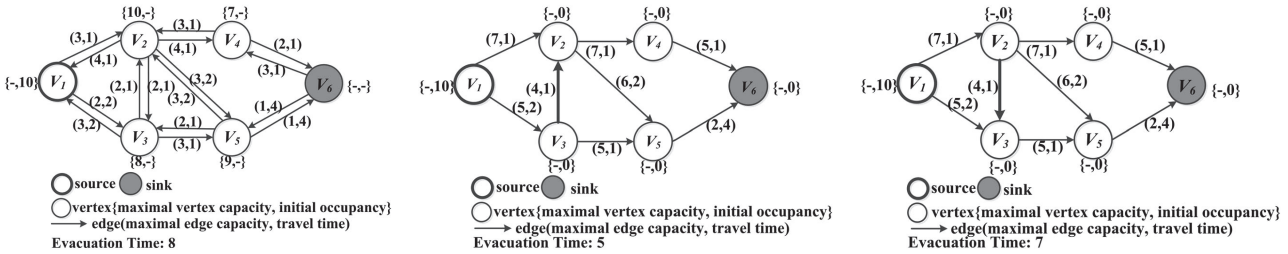

(a) Original network (b) Evacuation planning 1 (c) Evacuation planning 2

Figure 2: An evacuation scenario and two contraflow-based evacuation plans.

$f(r)$ is used to calculate the maximal traffic flow of route r under capacity constraints of vertices and edges and is expressed in (3). $V_{n,cap}^{t_n}$ denotes the available residual capacities of vertex V_n on route r at its arrival time t_n, where $t_n = ts + \sum_{l=1}^{n} e_{traT}^{\langle V_{l-1}, V_l \rangle}$, and $e_{cap}^{(\langle V_{n-1}, V_n \rangle, t_{n-1})}$ denotes the available residual capacity of edge $e^{\langle V_{n-1}, V_n \rangle}$ on route r at its arrival time t_{n-1}.

$$f(r) = \min \begin{cases} V_{0,Occ} \\ V_{n,cap}^{t_n} \\ e_{cap}^{(\langle V_{n-1}, V_n \rangle, t_{n-1})} \end{cases} \tag{3}$$

$$\text{s.t.} \quad \forall e^{\langle V_{n-1}, V_n \rangle} \in r,\ V_n \in r,\ 1 \le n \le N$$

Formula (1) illustrates the capacity constraints along the time dimension during evacuation. Constraint ① ensures that the outflow of source vertex V_s does not exceed the initial occupancy of source vertex V_s. Constraint ② enforces that the inflow of the sink vertices must be equal to the initial occupancy of the source vertices. In addition, the model capacity of vertices and edges cannot be negative during evacuation due to Constraint ③.

3.2. Contraflow Problem. In a large transportation network, long distance traffic jams usually cover the roads when emergencies occur. Contraflow-based methods are considered effective techniques for remedying traffic congestion [2]. However, an appropriate contraflow reconfiguration is difficult to calculate. Generally, two main difficulties are encountered in calculating optimal contraflow reconfiguration: (1) it is NP-hard to find all possible combinations of edge directions and calculate the evacuation time of these contraflow combinations and (2) it is time-consuming to evaluate the effects of dynamic traffic flow on these contraflow reconfiguration candidates.

Figure 2 illustrates an evacuation scenario and two contraflow-based evacuation planning results. The evacuation time is 8 time units based on the original network configuration in Figure 2(a). Figures 2(b) and 2(c) illustrate two contraflow reconfigurations, which combine all the two-way edge directions and merge the edge capacities to increase the upper bound on the evacuation capacity. The contraflow reconfiguration in Figure 2(b) reduces the evacuation time to 5 time units, while the contraflow reconfiguration in Figure 2(c) reduces the evacuation time to 7 time units. The only difference between the two contraflow reconfigurations is the edge direction between vertex V_2 and vertex V_3. Thus, it is vital for an optimal contraflow reconfiguration to select the critical edges that affect evacuation performance and determine their ideal direction after reversal.

4. Proposed Algorithm

This paper proposes the CC-Adap algorithm, which heuristically evaluates the evacuation routes, and integrates it with a contraflow-based method for distributing the evacuation routes with the least traffic congestion and maximal flow rate to evacuees. In addition, CC-Adap reuses historical evacuation routes to reduce computational costs and accelerate the evacuation process. Algorithm 1 gives the pseudocode of the CC-Adap algorithm.

Step 0 (initialization). For a given network $G(V, E)$, let C be the to-be-reversed edge set, ts be the initial time step

Input: $G(V, E)$, $C \leftarrow \varnothing$, $ts = 0$, $RS \leftarrow \varnothing$, $HR \leftarrow \varnothing$
Output: RS and C
(1) **while** there are still evacuees in source vertices **do**
(2) $r \leftarrow$ GetEvaRoute(G, ts);
(3) **if** r is not available **then**
(4) ts++; HRouteReuse(G, HR, ts);
(5) **else**
(6) $\delta = -1$; //Set initial value of δ
(7) δ =RouteEvaluation(G, HR, ts, r);
(8) **if** $\delta == -1$ **then** $\delta = 1$; //Exceptional case
(9) **else**
(10) **if** $\delta == 1$ **then**
(11) $c \leftarrow$ ContraflowReconfiguration(G, r);
(12) NetworkUpdate(G, ts, r);
(13) $C \leftarrow C \cup c$;
(14) $r.\rho = 0$;
(15) $RS \leftarrow RS \cup r$;
(16) $HR \leftarrow HR \cup r$;
(17) **end if**
(18) **end if**
(19) **end if**
(20) **end while**

Algorithm 1: CC-Adap algorithm.

when evacuees leave source vertices, RS be the to-be-solved evacuation planning route set, and HR be the historical evacuation route set.

Step 1 (GetEvaRoute). CC-Adap utilizes the evacuation route generation method in the Max-Flow Rate Priority (MFRP) algorithm [31] to select optimal candidate route r from among the available routes from source vertices to the nearest sink vertices. MFRP introduces parameter *FlowRate* to describe the route capacity. The formula of *FlowRate* is shown in (4).

$$FlowRate = \frac{f(r)}{c(r)} \tag{4}$$

The main strategy of the MFRP algorithm [31] is to calculate the available candidate routes by Dijkstra algorithm and balance the number of transferred evacuees with the travel time to select evacuation routes with maximal *FlowRate*. The performance of MFRP has been analyzed in [31]. CC-Adap guarantees the shortest possible evacuation time by employing MFRP [31] to select the optimal candidate routes.

Step 2 (RouteEvaluation). The use of low-quality routes might aggravate traffic congestion and increase the total evacuation time. CC-Adap introduces a parameter rq for quantizing route r, which is generated in Step 1, and historical evacuation route to avoid selecting lower-quality evacuation routes. The formula of rq is presented in

$$rq = \min\left(\frac{V_{s,Occ}}{f(r')}, c(r) - c(r')\right) * \left(f(r) - f(r')\right) \tag{5}$$

where r' is the historical evacuation route in HR, which has the same source vertex as r. Equation (5) represents the evacuation capability gap between routes r and r' when they evacuate evacuees at same times under the same traffic conditions.

The *RouteEvaluation* function operates as follows: First, we introduce parameter δ for reserving the evaluation result and set $\delta = -1$ initially. For each historical evacuation route r' in HR, we evaluate rq between r and r' by employing (5), where r and r' have the same source vertex, and reserve the evaluation result using δ as follows, which is expressed in (6): If rq is less than zero, then we set $\delta = 0$ and calculate the next historical evacuation route r' in HR. Otherwise, r is suitable for evacuation and we set $\delta = 1$ and terminate the evaluation procedure. If there is no route with the same source vertex as r in HR, we assume that r can also be used for evacuation and set $\delta = 1$.

$$\delta = \begin{cases} 0 & rq < 0 \\ 1 & rq \geq 0 \end{cases} \tag{6}$$

Step 3 (ContraflowReconfiguration). Greedy method can be used in evacuation route planning [2]. The appropriate contraflow strategy can be determined using Greedy method which has the advantage of obtaining the global optimal solution by local optimal solution. Thus, CC-Adap integrates Greedy method and iterative optimization technique to reverse the two-way edges on the evacuation routes iteratively in this paper. However, the edges on the evacuation routes cannot be reversed repeatedly as long as the edges have been flipped. The modified edge direction of the to-be-reversed edges depends on the traffic flow along the evacuation routes. The upper bound on the capacity of the flipped edges is increased by merging the two-way edges. The travel time of

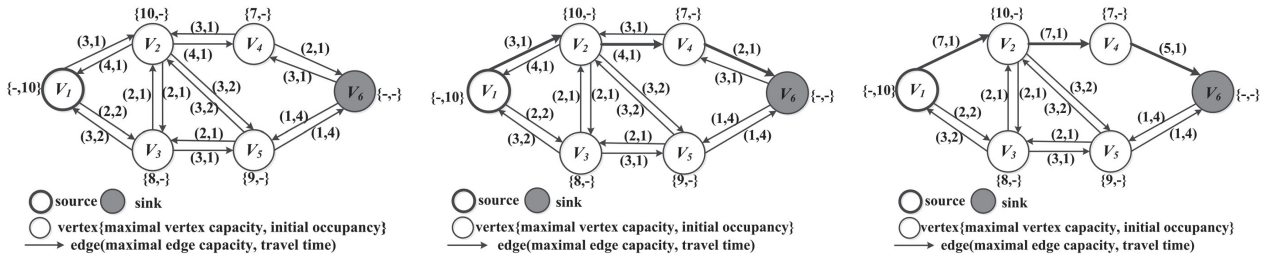

(a) Original network (b) Select evacuation route (c) Contraflow result

Figure 3: Example of the proposed contraflow-based method.

the reversed edges is equal to that of the two-way edges, which have the same edge direction as the flipped edges.

Figure 3 illustrates the steps for implementing the proposed contraflow reconfiguration method. Figure 3(a) is the original network configuration. In Figure 3(b), we select evacuation route $\langle V_1 - V_2 - V_4 - V_6\rangle$. Its traffic flow is $\min\{10, 3, 10, 4, 7, 2, \infty\} = 2$. As shown in Figure 3(c), the two-way edges on this route are merged and the maximal capacity of the flipped edges is increased. After contraflow reconfiguration, the traffic flow is increased to $\min\{10, 7, 10, 7, 7, 5, \infty\} = 5$. Thus, the evacuation capability of route $\langle V_1 - V_2 - V_4 - V_6\rangle$ is improved.

Step 4 (NetworkUpdate). After evacuees are transferred from source vertex to sink vertex, the available residual capacities of transition vertices and edges along route r are updated in (7) and (8), respectively, and the source vertex's residual evacuees of route r are updated in (9).

$$V_{n,cap}^{t_n} = V_{n,cap}^{t_n} - f(r) \quad V_n \in r \tag{7}$$

$$e_{cap}^{(\langle V_{n-1},V_n\rangle,t_{n-1})} = e_{cap}^{(\langle V_{n-1},V_n\rangle,t_{n-1})} - f(r) \quad e^{\langle V_{n-1},V_n\rangle} \in r \tag{8}$$

$$V_{0,Occ} = V_{0,Occ} - f(r) \quad V_0 \in r \tag{9}$$

Based on (7), (8), and (9), the traffic conditions can be monitored in real time for the next-iteration route calculation.

Step 5 (HRouteReuse). When there is no available evacuation route at the current time step, CC-Adap proceeds to the next time step (ts++) and returns to Step 1 to calculate routes. Before calculating routes, CC-Adap reuses historical evacuation routes in HR to reduce the computational cost and accelerate the evacuation process. To avoid evacuating along the same evacuation routes continually, CC-Adap introduces a parameter ρ that marks historical evacuation route hr in HR if hr is reserved at the last time step. ρ is defined in

$$\rho = \begin{cases} 0 & hr \text{ is reserved last time step} \\ 1 & hr \text{ isn't reserved last time step} \end{cases} \tag{10}$$

The *HRouteReuse* function operates as follows: For each historical evacuation route hr in HR, if $f(hr) = 0$ under the current traffic conditions, it will be excluded from HR. Otherwise, if the corresponding ρ is equal to 0, hr is reserved at the last time step and is not suitable for evacuation at the current time step, we set $\rho = 1$ for the next iteration. If ρ is equal to 1, then hr is used for evacuation at the current time step and traffic conditions are updated by Step 4.

In each iteration, the generated route r in Step 1 is reserved in HR and RS when r is used to transfer evacuees and ρ of r is set to 0. Meanwhile, the to-be-reversed edges on route r are reserved in C. To complete the evacuation, Steps 1–5 can be repeated until there is no evacuee who needs to be evacuated.

5. Experiment

5.1. Experimental Design. There are many evacuation algorithms that can provide evacuation route planning, such as the classical CCRP algorithm [1], LRP algorithm [17], MR algorithm [31], MFRP algorithm [31], and Greedy algorithm [2]. Reference [31] has validated that the performance of MFRP algorithm is better than LRP and MR. Besides, Greedy algorithm is a classical contraflow evacuation algorithm. CC-Adap algorithm integrates MFRP algorithm and Greedy algorithm in this paper. Thus, CCRP, MFRP, and Greedy algorithms are selected to validate the performance of CC-Adap algorithm.

5.2. Experiment Data. In this paper, we use the following notations to describe evacuation situations: n is the number of vertices, s is the number of source and sink vertices, m is the number of edges, and p is the number of evacuees. The experimental data that are used in this paper is generated by the network simulator tool NETGEN [32]. However, NETGEN does not generate the maximal vertex capacity for transition vertices. This paper uses a random number generation function, namely, *rand()*, to generate the maximal vertex capacity for transition vertices in (11). The seed of the *rand()* function is set to the vertex number to avoid generating the same networks. α and β are two coefficients in (11), which imply that the lower bound on the edge capacity is β and the upper bound on the edge capacity is $(rand()\%((\alpha * p)/s)) + \beta$. α and β can be reset according to the practical requirements. In this paper, we set $\alpha = 3$ and $\beta = 20$ [31].

$$V_{i,MCap} = \left(rand()\,\%\frac{\alpha * p}{s}\right) + \beta \quad V_i \in V_M \tag{11}$$

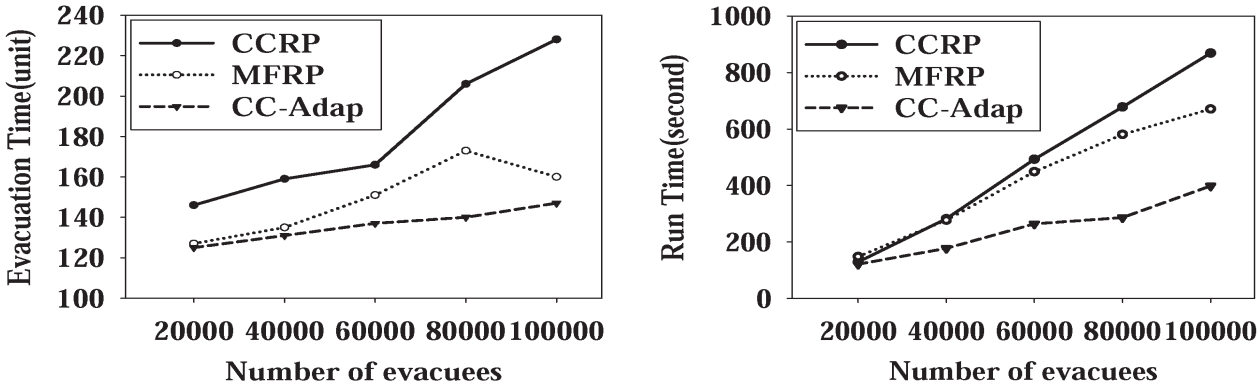

(a) $n = 256$; $m = 768$; $s = 26$ (b) $n = 256$; $m = 768$; $s = 26$

Figure 4: Evacuation quality in a small transportation network.

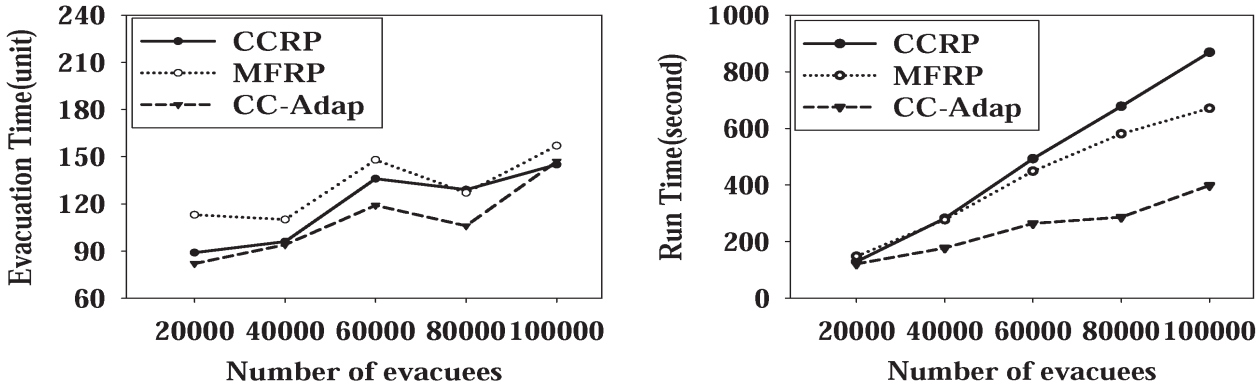

(a) $n = 1024$; $m = 5258$; $s = 102$ (b) $n = 1024$; $m = 5258$; $s = 102$

Figure 5: Evacuation quality in a large transportation network.

5.3. Experimental Result

5.3.1. Feasibility Verification. The purpose of this section is to evaluate the feasibility of using CC-Adap in evacuation planning. CC-Adap is compared with CCRP and MFRP to determine whether CC-Adap can be used for evacuation planning and to optimize evacuation plans by applying a contraflow-based method.

In this section, two experiments are carried out. Each experiment has five test groups and the number of vertices, edges, source, and sink vertices is fixed. We vary the number of evacuees from 20000 to 100000. Figures 4 and 5 depict the results on the evacuation time and run time of the three algorithms in small-scale and large-scale transportation networks, respectively. According to Figure 4(a), CC-Adap has the smallest and nearly linearly growing evacuation time with the increase of the number of evacuees, while CCRP and MFRP have steeply increasing evacuation time and the evacuation time of CCRP is almost double that of CC-Adap. The run time of CCRP and MFRP grows rapidly as the number of evacuees increases, while CC-Adap has a stable run time and the run time of CCRP and MFRP is more than twice that of CC-Adap when the number of evacuees is 100000 in Figure 4(b). As shown in Figure 5, CC-Adap has the shortest evacuation time with the increase in the number of evacuees in Figure 5(a), followed by CCRP, and MFRP has the longest evacuation time. In terms of the run time, CC-Adap, CCRP, and MFRP all show nearly linear growth with the increase in the number of evacuees, and CC-Adap has a run time that is nearly half those of CCRP and MFRP.

5.3.2. Scalability Verification. The purpose of this section is to evaluate the scalability of CC-Adap to complex evacuation situations and CC-Adap is compared with CCRP, MFRP, and Greedy algorithms.

Comparison on Networks with Different Number of Edges. Figure 6 plots the experimental results in terms of evacuation time and run time of the four algorithms against the number of edges. This experiment is carried out with five subexperiments. The number of vertices is fixed at 256, and

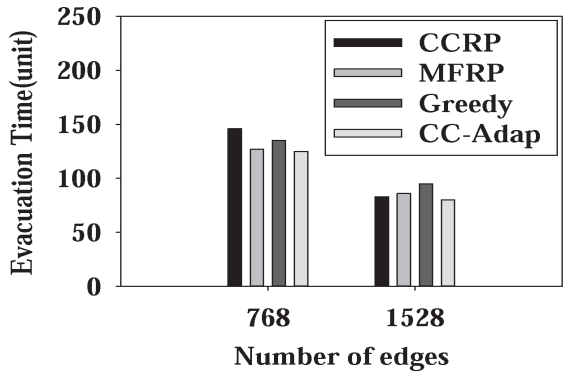

(a) $n = 256$; $s = 26$; $p = 20000$

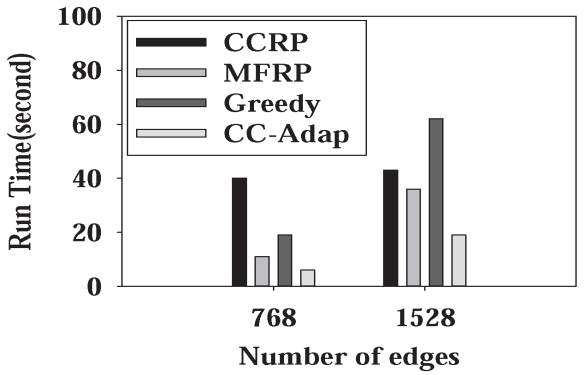

(b) $n = 256$; $s = 26$; $p = 20000$

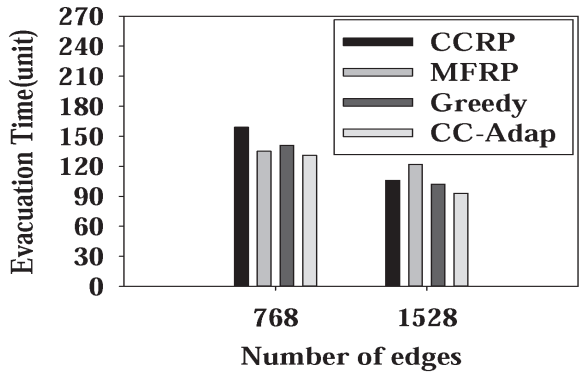

(c) $n = 256$; $s = 26$; $p = 40000$

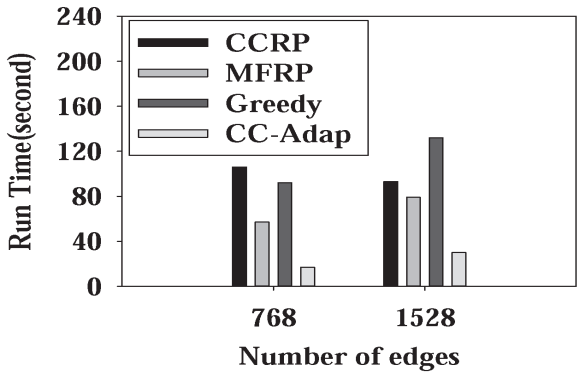

(d) $n = 256$; $s = 26$; $p = 40000$

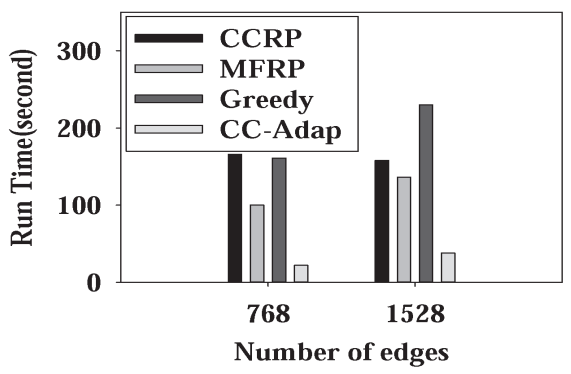

(e) $n = 256$; $s = 26$; $p = 60000$

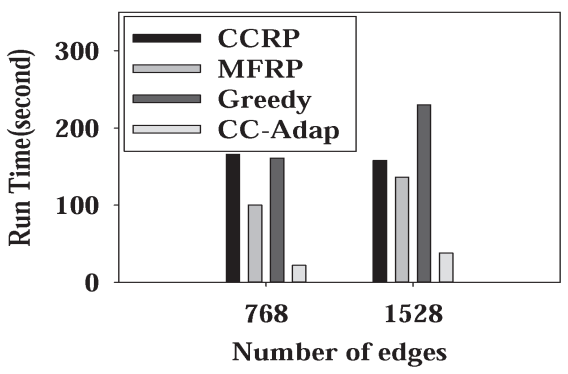

(f) $n = 256$; $s = 26$; $p = 60000$

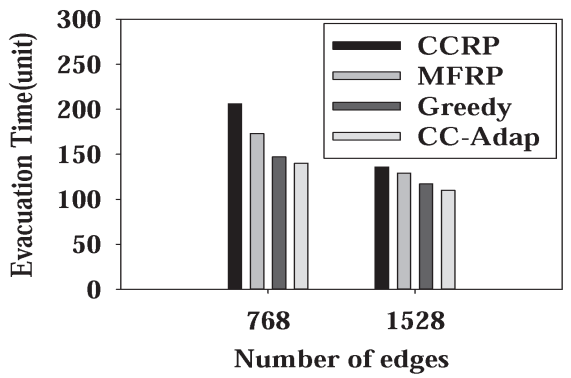

(g) $n = 256$; $s = 26$; $p = 80000$

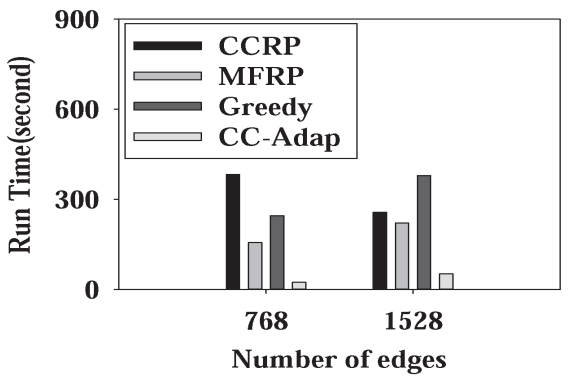

(h) $n = 256$; $s = 26$; $p = 80000$

Figure 6: Continued.

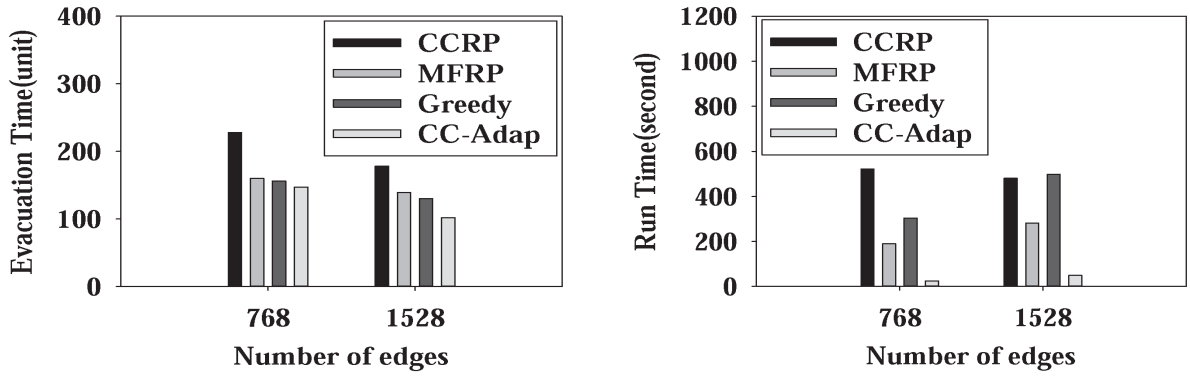

(i) $n = 256$; $s = 26$; $p = 100000$ (j) $n = 256$; $s = 26$; $p = 100000$

Figure 6: Evacuation quality with respect to the number of edges.

the number of source and sink vertices is fixed at 26. The number of evacuees is varied from 20000 to 100000. Each subexperiment has two test groups and the number of edges is varied from 768 to 1528. According to Figure 6, CC-Adap has the shortest evacuation time in each subexperiment as the number of edges varies. In addition, CC-Adap shows the minimum change in evacuation time when the number of edges varies, followed by Greedy, MFRP, and CCRP. Regarding the run time of these four algorithms when the number of edges varies, as shown in Figure 6, CC-Adap has the shortest run time comparing with the CCRP, MFRP, and Greedy algorithms; the run time of CC-Adap is less than 20 percent of those of CCRP and Greedy. In addition, the number of edges has little effect on the run time of CC-Adap, while the CCRP, MFRP, and Greedy algorithms are affected by the variation of the number of edges.

Comparison on Different Number of Evacuees. Figure 7 plots the experimental results on evacuation time and run time of the four algorithms against the number of evacuees. This experiment is carried out with three subexperiments, and the numbers of vertices, edges, and source and sink vertices are fixed. Each subexperiment has five test groups and the number of evacuees is varied from 20000 to 100000. According to Figure 7, the evacuation time of CC-Adap increases (perhaps linearly) with the increase in the number of evacuees, while CCRP has a steeply increasing evacuation time, MFRP and Greedy show volatility growth of evacuation time with the increase in the number of evacuees. In particular, according to Figures 7(c) and 7(e), the evacuation time of CC-Adap is almost 50 percent those of CCRP, MFRP, and Greedy when tackling a massive number of evacuees. Moreover, CC-Adap has a short and stable run time with the increase in the number of evacuees, while the CCRP, MFRP, and Greedy algorithms have steeply, perhaps superlinearly, increasing run time. The run time of CC-Adap is almost 10 percent that of the Greedy algorithm in Figures 7(b), 7(d), and 7(f) and that of CCRP in Figures 7(b) and 7(d) when tackling a massive number of evacuees.

Comparison on Different Numbers of Source and Sink Vertices. Figure 8 plots the experimental results on the evacuation time and run time of the four algorithms against the number of source and sink vertices. This experiment is carried out with five subexperiments. The number of vertices is fixed at 256, the number of edges is fixed at 1528, and the number of evacuees is varied from 20000 to 100000. Each subexperiment has two test groups and the number of source and sink vertices is varied from 26 to 52. According to Figure 8, CC-Adap produces the solutions with shortest evacuation time comparing with the CCRP, MFRP, and Greedy algorithms when the number of source and sink vertices is varied. In addition, the evacuation time of CC-Adap has the slowest increase with the increase in the number of source and sink vertices comparing with the other three algorithms. For different number of source and sink vertices, CC-Adap has the fastest run time comparing with the CCRP, MFRP, and Greedy algorithms. As the number of source and sink vertices varies from 26 to 52, the run time of the MFRP and Greedy algorithms rises steeply, CCRP shows a small growth in run time, and CC-Adap shows the smallest increase in run time.

Comparison on Large Transportation Networks. Figure 9 depicts the experimental results of the four algorithms in terms of evacuation time and run time on a large-scale transportation network. The experiment is carried out with five test groups and has a fixed network configuration of 1024 vertices, 5258 edges, and 102 source and sink vertices. We vary the number of evacuees from 20000 to 100000 to test the algorithms' performances. As shown in Figure 9(a), CC-Adap can generate high-quality evacuation solutions with the shortest evacuation time when the number of evacuees grows in a large-scale transportation network. Moreover, the run time of CC-Adap shown in Figure 9(b) also has the smallest and most stable growth with different number of evacuees in large-scale transportation network evacuation scenarios. In addition, CC-Adap has the minimum growth ratio of run

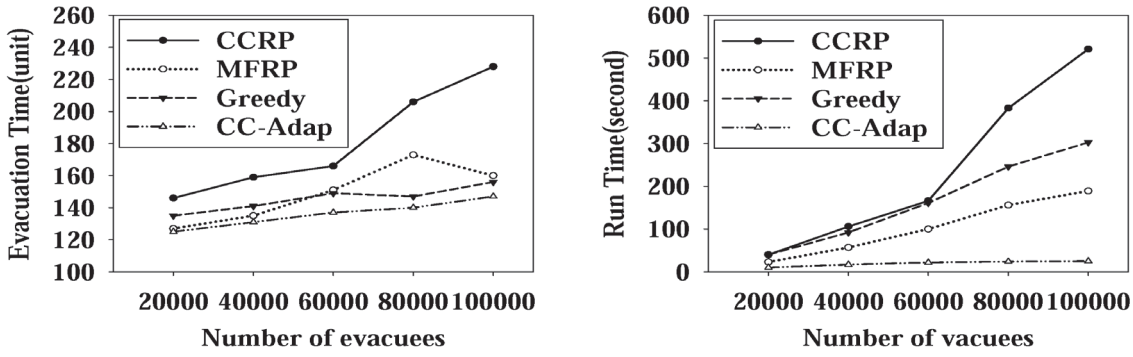

(a) $m = 768$; $n = 256$; $s = 26$

(b) $m = 768$; $n = 256$; $s = 26$

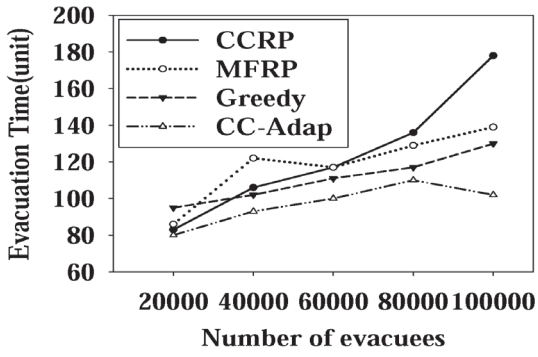

(c) $m = 1528$; $n = 256$; $s = 26$

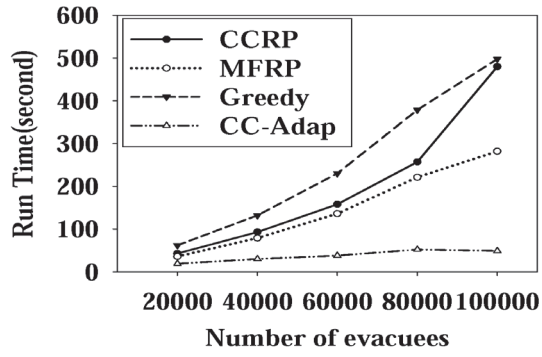

(d) $m = 1528$; $n = 256$; $s = 26$

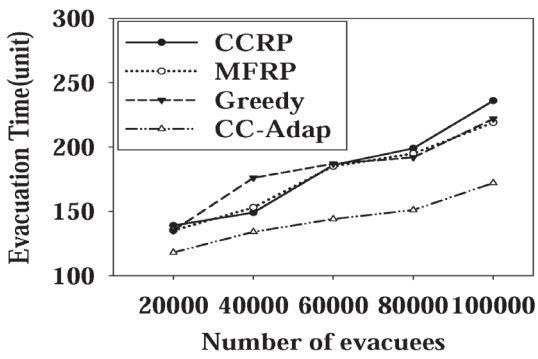

(e) $m = 1528$; $n = 256$; $s = 52$

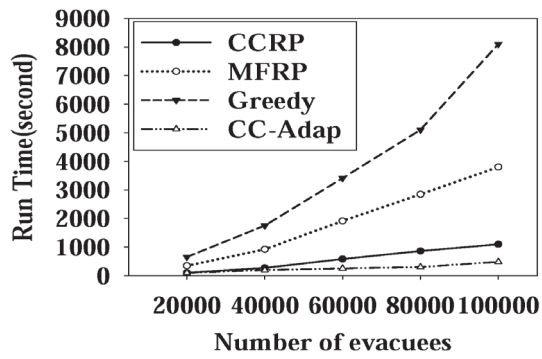

(f) $m = 1528$; $n = 256$; $s = 52$

Figure 7: Evacuation quality with respect to the number of evacuees.

time with the increase in the number of evacuees, comparing with CCRP, MFRP, and Greedy (which have growth ratios of nearly 50 percent).

5.4. Summary of Experiments. There are many dynamic factors that are critical to the transportation network, such as number of evacuees and affected areas, which makes evacuation management a daunting task. These dynamic factors can be evaluated systematically by building appropriate evacuation models [33]. Only by taking these factors into consideration we can optimize evacuation management. This section will discuss these dynamic factors and evaluate the optimality of the CC-Adap algorithm based on the experimental results.

(i) **Number of edges**: the more edges there are, the more difficult it is to find appropriate routes to evacuate evacuees. CC-Adap can intelligently evaluate the routes to choose the optimal one for evacuation, thereby making it more scalable with the number of edges.

(ii) **Number of source and sink vertices**: an increase in the number of source and sink vertices in a transportation network means that the evacuees are

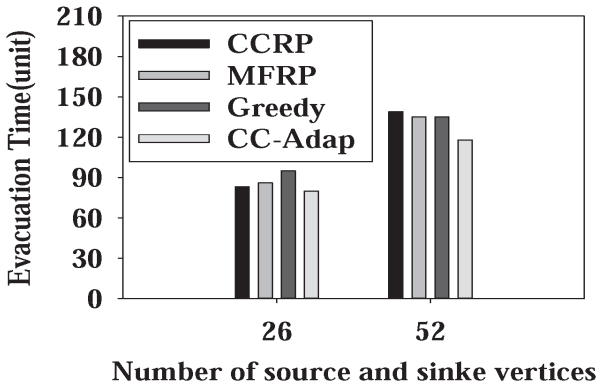

(a) $n = 256$; $m = 1528$; $p = 20000$

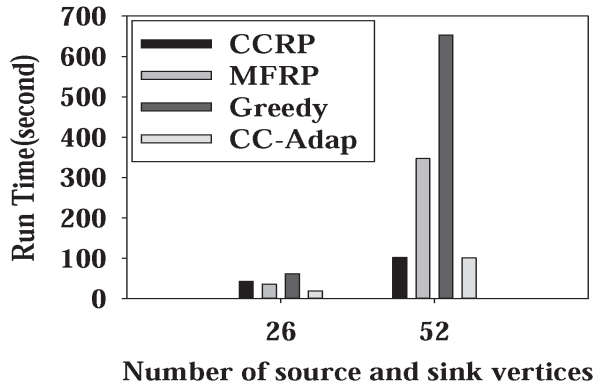

(b) $n = 256$; $m = 1528$; $p = 20000$

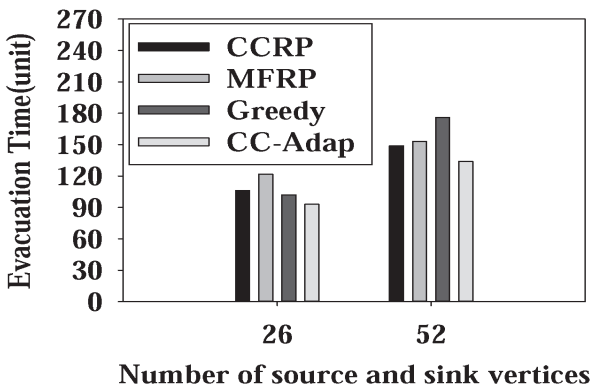

(c) $n = 256$; $m = 1528$; $p = 40000$

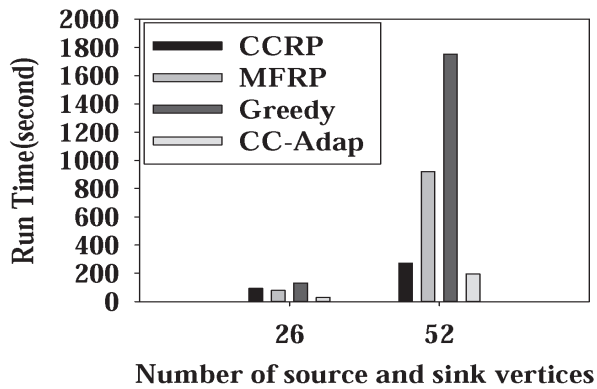

(d) $n = 256$; $m = 1528$; $p = 40000$

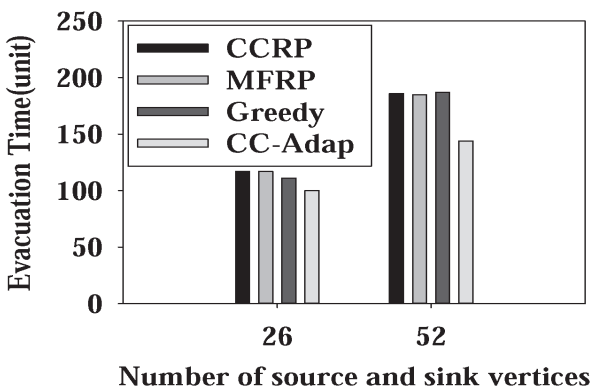

(e) $n = 256$; $m = 1528$; $p = 60000$

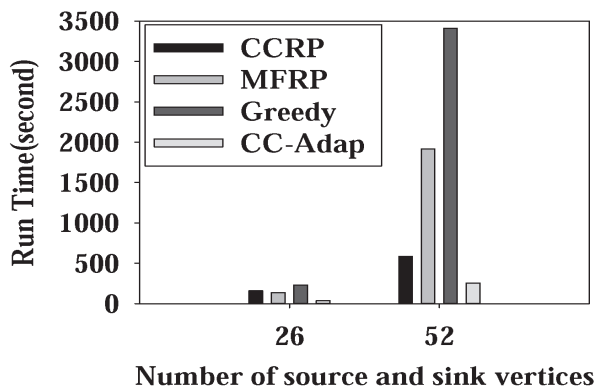

(f) $n = 256$; $m = 1528$; $p = 60000$

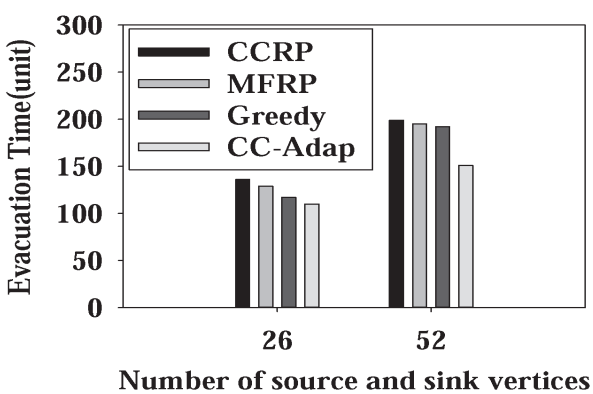

(g) $n = 256$; $m = 1528$; $p = 80000$

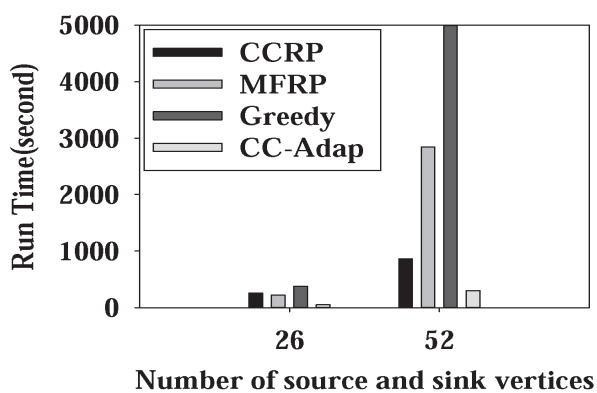

(h) $n = 256$; $m = 1528$; $p = 80000$

Figure 8: Continued.

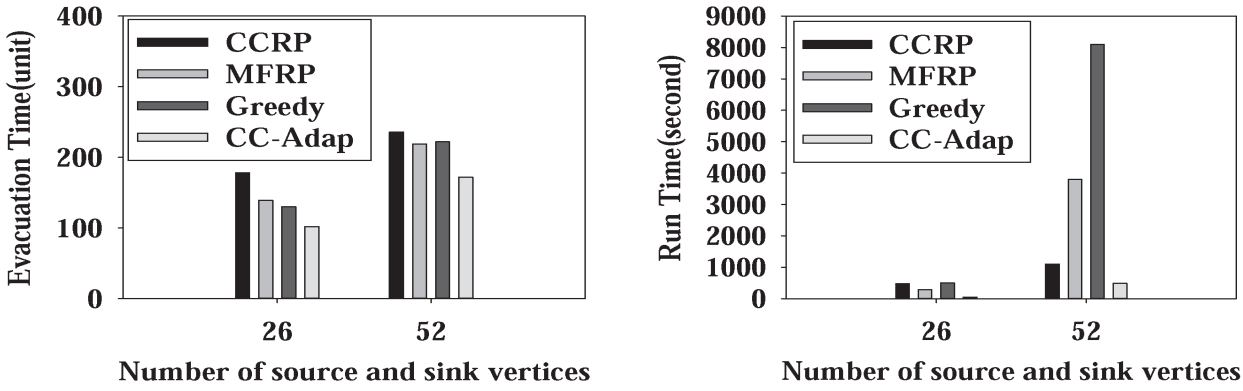

(i) $n = 256; m = 1528; p = 100000$ (j) $n = 256; m = 1528; p = 100000$

Figure 8: Evacuation quality with respect to the number of source and sink vertices.

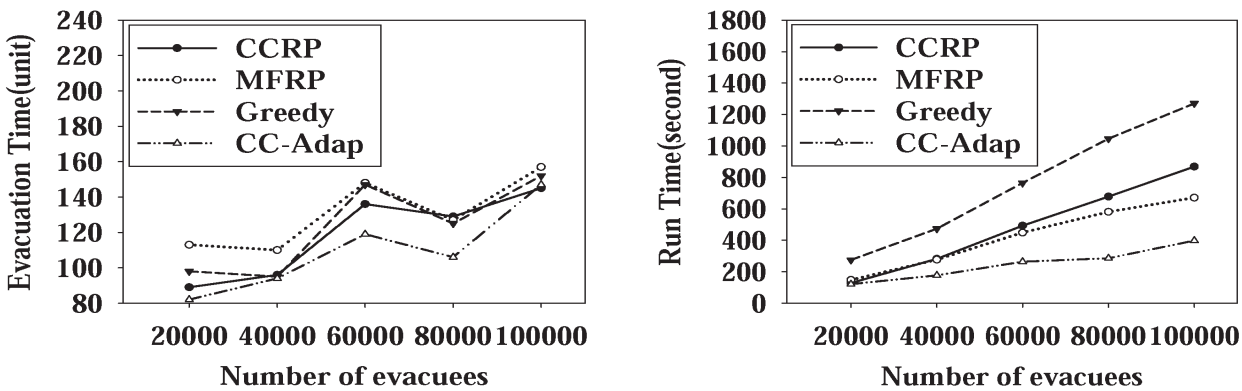

(a) $n = 1024; s = 102; m = 5258$ (b) $n = 1024; s = 102; m = 5258$

Figure 9: Evacuation quality of large-scale transportation network evacuation.

more scattered in the network [1]. It might lead to difficulty in calculating the evacuation routes. CC-Adap reuses the historical evacuation routes to reduce the computational costs, thereby making CC-Adap more scalable with the number of source and sink vertices.

(iii) **Number of evacuees**: capacity constraints are the major limiting factor in optimizing an evacuation strategy. Traffic congestion occurs easily when there are too many evacuees. CC-Adap applies a contraflow-based method to improve the performance of evacuation routes, which makes CC-Adap more scalable with the number of evacuees.

(iv) **Traffic scale**: large and complex urban evacuation problems cause most evacuation route planning approaches to fail. CC-Adap integrates an iterative optimization technique and a contraflow-based method to optimize an evacuation plan, thereby making CC-Adap more effective in addressing urban evacuation planning.

6. Conclusions

This paper presents a heuristic contraflow reconfiguration evacuation algorithm, which is called Capacity-Constrained Contraflow Adaption algorithm. CC-Adap can heuristically evaluate evacuation routes to assign high-quality routes to evacuees. Moreover, the proposed contraflow-based method is applied to reconfigure evacuation routes to reduce traffic congestion and improve evacuation performance. Meanwhile, CC-Adap reuses historical evacuation routes to reduce computational costs and accelerate the evacuation process. Experimental results have shown that the CC-Adap algorithm can optimize evacuation route planning in terms of evacuation time and run time.

However, more research is required for CC-Adap. First, a more effective evacuation route generation method should be constructed. Second, the evaluation method should be improved to evaluate the evacuation routes more effectively.

Data Availability

The data used to support the findings of this study are available from the first author.

Conflicts of Interest

The authors declare that they have no conflicts of interest.

Acknowledgments

This work is supported by the National Key Research and Development Program of China (no. 2016YFB0502600) and the National Natural Science Foundation of China (no. 41701594).

References

[1] Q. Lu, B. George, and S. Shekhar, "Capacity constrained routing algorithms for evacuation planning: A summary of results," in *Proceedings of the International Symposium on Spatial and Temporal Databases*, pp. 291–307, Berlin, Germany, 2005.

[2] S. Kim, S. Shekhar, and M. Min, "Contraflow transportation network reconfiguration for evacuation route planning," *IEEE Transactions on Knowledge and Data Engineering*, vol. 20, no. 8, pp. 1115–1129, 2008.

[3] J. W. Wang, H. F. Wang, W. J. Zhang, W. H. Ip, and K. Furuta, "Evacuation planning based on the contraflow technique with consideration of evacuation priorities and traffic setup time," *IEEE Transactions on Intelligent Transportation Systems*, vol. 14, no. 1, pp. 480–485, 2013.

[4] T. Takabatake, T. Shibayama, M. Esteban, H. Ishii, and G. Hamano, "Simulated tsunami evacuation behavior of local residents and visitors in Kamakura, Japan," *International Journal of Disaster Risk Reduction*, vol. 23, pp. 1–14, 2017.

[5] K. Shahabi and J. P. Wilson, "CASPER: Intelligent capacity-aware evacuation routing," *Computers, Environment and Urban Systems*, vol. 46, pp. 12–24, 2014.

[6] S. Kim, B. George, and S. Shekhar, "Evacuation route planning: scalable heuristics," in *Proceedings of the 15th annual ACM international symposium on Advances in geographic information systems*, p. 20, 2007.

[7] M. Jha, K. Moore, and B. Pashaie, "Emergency evacuation planning with microscopic traffic simulation," *Transportation Research Record*, no. 1886, pp. 40–48, 2004.

[8] M. Fellendorf and P. Vortisch, "Microscopic traffic flow simulator VISSIM," in *Fundamentals of traffic simulation*, pp. 63–93, Springer, New York, NY, USA, 2010.

[9] G. Lämmel, D. Grether, and K. Nagel, "The representation and implementation of time-dependent inundation in large-scale microscopic evacuation simulations," *Transportation Research Part C: Emerging Technologies*, vol. 18, no. 1, pp. 84–98, 2010.

[10] Y.-T. Hsu and S. Peeta, "Clearance Time Estimation for Incorporating Evacuation Risk in Routing Strategies for Evacuation Operations," *Networks and Spatial Economics*, vol. 15, no. 3, pp. 743–764, 2015.

[11] V. Zyryanov and A. Feofilova, "Simulation of Evacuation Route Choice," *Transportation Research Procedia*, vol. 20, pp. 740–745, 2017.

[12] X. Pan, C. S. Han, K. Dauber, and H. H. Law, "A multi-agent based framework for the simulation of human and social behaviors during emergency evacuations," *Ai & Society*, vol. 22, no. 2, pp. 113–132, 2007.

[13] G.-Y. Wu and H.-Ch. Huang, "Modeling the emergency evacuation of the high rise building based on the control volume model," *Safety Science*, vol. 73, no. 5, pp. 62–72, 2015.

[14] D.-J. Noh, J. Koo, and B.-I. Kim, "An efficient partially dedicated strategy for evacuation of a heterogeneous population," *Simulation Modelling Practice and Theory*, vol. 62, pp. 157–165, 2016.

[15] A. Beloglazov, M. Almashor, E. Abebe, J. Richter, and K. C. B. Steer, "Simulation of wildfire evacuation with dynamic factors and model composition," *Simulation Modelling Practice and Theory*, vol. 60, pp. 144–159, 2016.

[16] S. Yuan, S. A. Chun, B. Spinelli, Y. Liu, H. Zhang, and N. R. Adam, "Traffic evacuation simulation based on multi-level driving decision model," *Transportation Research Part C: Emerging Technologies*, vol. 78, pp. 129–149, 2017.

[17] M. Zeng and C. Wang, "Evacuation route planning algorithm: Longer route preferential. International Symposium on Neural Networks," in *Proceedings of the International Symposium on Neural Networks*, pp. 1062–1071, Berlin, Germany, 2009.

[18] W. Kang, F. Zhu, Y. Lv, G. Xiong, L. Xie, and B. Xi, "A heuristic implementation of emergency traffic evacuation in urban areas," in *Proceedings of the 2013 IEEE International Conference on Service Operations and Logistics, and Informatics, SOLI 2013*, pp. 40–44, chn, July 2013.

[19] M. U. S. Khan, O. Khalid, Y. Huang et al., "MacroServ: A Route Recommendation Service for Large-Scale Evacuations," *IEEE Transactions on Services Computing*, vol. 10, no. 4, pp. 589–602, 2017.

[20] E. Pourrahmani, M. R. Delavar, and M. A. Mostafavi, "Optimization of an evacuation plan with uncertain demands using fuzzy credibility theory and genetic algorithm," *International Journal of Disaster Risk Reduction*, vol. 14, pp. 357–372, 2015.

[21] L.-W. Chen, J.-H. Cheng, and Y.-C. Tseng, "Distributed Emergency Guiding with Evacuation Time Optimization Based on Wireless Sensor Networks," *IEEE Transactions on Parallel and Distributed Systems*, vol. 27, no. 2, pp. 419–427, 2016.

[22] Y. Ikeda and M. Inoue, "An Evacuation Route Planning for Safety Route Guidance System after Natural Disaster Using Multi-objective Genetic Algorithm," in *Proceedings of the 20th International Conference on Knowledge Based and Intelligent Information and Engineering Systems, KES 2016*, pp. 1323–1331, gbr, September 2016.

[23] M. Heydar, J. Yu, Y. Liu, and M. E. H. Petering, "Strategic evacuation planning with pedestrian guidance and bus routing: a mixed integer programming model and heuristic solution," *Journal of Advanced Transportation*, vol. 50, no. 7, pp. 1314–1335, 2016.

[24] U. Pyakurel, T. N. Dhamala, and T. N. Dhamala, "Models and algorithms on contraflow evacuation planning network problems," *International Journal of Operations Research*, vol. 12, no. 2, pp. 36–46, 2015.

[25] U. Pyakurel and T. N. Dhamala, "Continuous Dynamic Contraflow Approach for Evacuation Planning," *Annals of Operations Research*, vol. 253, no. 1, pp. 573–598, 2017.

[26] U. Pyakurel and T. N. Dhamala, "Continuous Time Dynamic Contraflow Models and Algorithms," *Advances in Operations Research*, vol. 2016, Article ID 7902460, 7 pages, 2016.

[27] J. Zhao, Y. Liu, and P. Li, "A network enhancement model with integrated lane reorganization and traffic control strategies," *Journal of Advanced Transportation*, vol. 50, no. 6, pp. 1090–1110, 2016.

[28] C. Xie, D.-Y. Lin, and S. Travis Waller, "A dynamic evacuation network optimization problem with lane reversal and crossing elimination strategies," *Transportation Research Part E: Logistics and Transportation Review*, vol. 46, no. 3, pp. 295–316, 2010.

[29] C. Even, V. Pillac, and P. Van Hentenryck, "NICTA evacuation planner: Actionable evacuation plans with contraflows," *Frontiers in Artificial Intelligence and Applications*, vol. 263, pp. 1143–1148, 2014.

[30] D. R. Fulkerson, "Flows in networks," in *Recent advances in mathematical programming*, pp. 319–331, McGraw-Hill, New York, NY, USA, 1963.

[31] D. Guo, C. Gao, W. Ni, and X. Hu, "Max-Flow rate priority algorithm for evacuation route planning," in *Proceedings of the 1st IEEE International Conference on Data Science in Cyberspace, DSC 2016*, pp. 275–283, chn, June 2016.

[32] D. Klingman, A. Napier, and J. Stutz, "NETGEN: a program for generating large scale capacitated assignment, transportation, and minimum cost flow network problems," *Management Science*, vol. 20, no. 5, pp. 814–821, 1974.

[33] E. Ronchi, F. N. Uriz, X. Criel, and P. Reilly, "Modelling large-scale evacuation of music festivals," *Case Studies in Fire Safety*, vol. 5, pp. 11–19, 2016.